MedChemComm

RSC Publishing

CONCISE ARTICLE

View Article Online
View Journal | View Issue

Cite this: *Med. Chem. Commun.*, 2013, **4**, 432

The advantage of biosensor analysis over enzyme inhibition studies for slow dissociating inhibitors – characterization of hydroxamate-based matrix metalloproteinase-12 inhibitors

Thomas Gossas,†[a] Helena Nordström,[a] Ming-Hua Xu,[b] Zhi-Hua Sun,‡[c] Guo-Qiang Lin,[c] Hans Wallberg[d] and U. Helena Danielson*[a]

Received 7th September 2012
Accepted 19th December 2012

DOI: 10.1039/c2md20268a

www.rsc.org/medchemcomm

The kinetic characteristics of hydroxamate-based inhibitors of matrix metalloproteinase (MMP)-12 were explored using an SPR biosensor-based assay and enzyme inhibition analysis. These high-affinity inhibitors were shown to dissociate very slowly from the enzyme–inhibitor complex while a carboxylate analogue had a much faster dissociation rate, verifying the importance of the hydroxamate group for the slow dissociation. Progress curve enzyme inhibition analysis confirmed that the hydroxamate compounds but not the carboxylate compound acted as time-dependent inhibitors. The slow dissociation excluded steady-state estimation of IC_{50}-values and K_i values but also made K_i values from progress curve analysis unreliable. Although a full characterization of the inhibitors using biosensor analysis was limited by slow dissociation, it provided kinetic and mechanistic information of relevance for MMP drug discovery and avoided some pitfalls of conventional enzyme inhibition assays.

Introduction

Our understanding of structure–activity relationships is still very much founded on equilibrium-based data, *e.g.* affinity (K_D) or IC_{50}, while the structural features that result in fast association or slow dissociation are not well understood. It is difficult to obtain such information with conventional enzyme inhibition assays and the fact that many lead compounds interact with slow kinetics is often not recognized. The advantage of a time-resolved direct binding assay for lead characterization is therefore emphasized in this study and discussed in comparison with conventional inhibition assays which often give misleading results for inhibitors with slow kinetics.

Matrix metalloproteinase (MMP)-12[a] is a metallo endopeptidase belonging to the matrixin subfamily M10A, according to the terminology used in the MEROPS database.[1] This family of enzymes is involved in extracellular tissue remodelling and thus influences processes like inflammation and cancer metastasis. The MMP family has for that reason attracted attention from many pharmaceutical and medical researchers. The specific interest in MMP-12 as a drug target has emerged as a consequence of its involvement in several major human diseases, for example chronic obstructive pulmonary disease (COPD) and rheumatoid arthritis.[2,3] The degradation of the extracellular matrix by this enzyme is an essential part of these diseases and MMP-12 inhibitors have therefore been expected to be suitable as drugs.

Potent MMP inhibitors can be designed by incorporating a zinc-binding group (ZBG), most commonly a hydroxamic acid moiety, into the inhibitor in a position where it makes a strong interaction with the catalytic zinc ion. For additional affinity and selectivity, interactions between the inhibitor and the S1′–S3′ pockets are also exploited. This approach has produced relatively small compounds with high affinity. Although several MMP inhibitors of this type have reached clinical trials, they have all failed due to severe side effects. Some of these effects are most likely due to inhibition of other MMPs and other metalloproteases, such as those of the ADAM-family.[4,5] It has been speculated that the ZBG contributes too much to the affinity so that discrimination among the MMP isoenzymes is very difficult to achieve.[6] This has seriously hampered the evolution of inhibitors to functioning drugs.[7] However, in order to fully understand the molecular basis of the poor specificity of ZBG-containing inhibitors, information about the kinetics of the interaction between these inhibitors and MMPs is required.

[a]*Department of Chemistry – BMC, Uppsala University, Box 576, SE-751 23, Uppsala, Sweden. E-mail: helena.danielson@kemi.uu.se; Fax: +46-18-558431; Tel: +46-18-471 4545*

[b]*Shanghai Institute of Materia Medica, Chinese Academy of Sciences, 555 Zuchongzhi Road, Shanghai 201203, China*

[c]*Shanghai Institute of Organic Chemistry, Chinese Academy of Sciences, 345 Lingling Road, Shanghai 200032, China*

[d]*Medivir AB, P.O. Box 1086, S-141 22 Huddinge, Sweden*

† Current address: Beactica AB, Box 567, SE-751 22 Uppsala, Sweden.

‡ Current address: College of Chemistry and Chemical Engineering, Shanghai University of Engineering Science, Shanghai 201600, China.

For this purpose, we used a set of drug-like inhibitors of MMPs (Fig. 1 and Scheme 1) and a time resolved SPR-based biosensor assay. The assay was originally developed for the identification of fragments binding to the active site of MMP-12 and used for screening of a fragment library.[8] Here it was used for the characterization of the interaction kinetics of effective inhibitors.

The present study confirmed that the hydroxamate group contributes significantly to the overall interaction with MMP-12 and that compounds of this class can act essentially as irreversible inhibitors of the enzyme, at least on the time scale of biochemical experiments. Although the slow dissociation can be an advantage for clinical efficacy, often discussed in terms of residence time, there may be disadvantages with respect to selectivity.

Results

Synthesis and selection of compounds

In order to have access to two compounds differing only in the zinc binding group, a compound with a carboxylate zinc binding group (**1** (ref. 8)), and a hydroxamate analogue (**2**), were synthesized according to the strategy outlined in Scheme 1. Two structurally unrelated, but also hydroxamate containing compounds, **3** (ref. 9) and **4** (ref. 10) were selected for comparison (Fig. 1). GM 6001 (**5**),[11,12] a hydroxamate-based MMP inhibitor tested in clinical trials against several types of diseases, was used as a well-known reference (Fig. 1).

Evaluation of inhibitory potency of studied compounds

As a starting point, the inhibitory potency of the compounds selected for this study was determined by a steady-state based enzyme inhibition assay using initial rate analysis (Table 1). It was confirmed that all compounds were inhibitory and had apparent affinities (K_i^{app}) ranging from 1 (**2**) to 50 nM (**1**). The parameter has been denoted "apparent" throughout this paper to point out that it is not a true equilibrium constant since the inhibition is not measured under strict equilibrium conditions (see below).

Development of a biosensor assay for characterization of MMP-12 inhibitors

In order to get further insights into the kinetics of the interactions and how they depended on the structural features of the compounds, a previously developed biosensor assay for MMP-12 (ref. 8) was adapted for kinetic characterization of inhibitors. An amine-coupling procedure, optimised for immobilization of MMP-12, was used to immobilize an amount of enzyme giving a signal of 2000–2500 RU. Compound **1** was selected for evaluation of the surface characteristics since it was found to bind reversibly, albeit with high affinity, and could be removed by mild regeneration conditions.

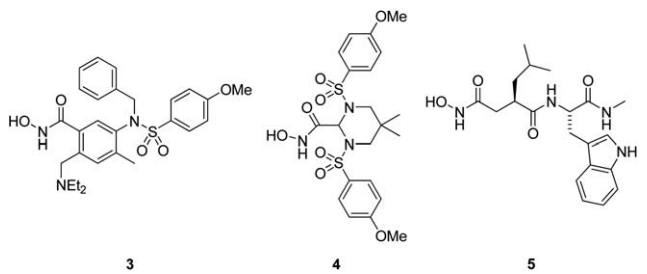

Fig. 1 Structures of compounds **3**, **4** and **5**.

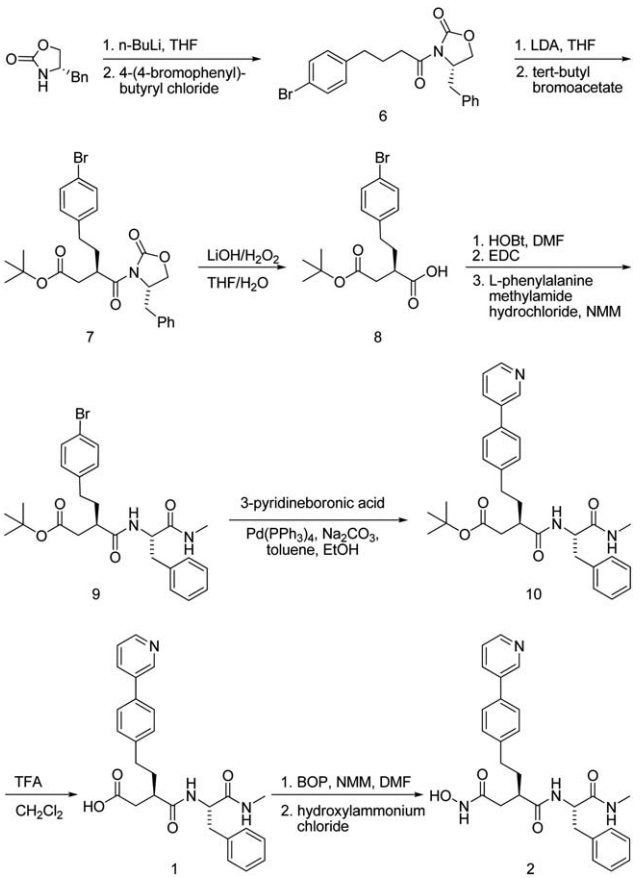

Scheme 1 General procedure for the preparation of compounds **1** and **2**.

Table 1 Inhibition and interaction kinetic parameters for studied MMP-12 inhibitors

	Initial rate analysis[a]	Progress curve analysis[b]		
Compound	K_i^{app} (nM)	k_{on} (10^5 M^{-1} s^{-1})	k_{off} (10^{-3} s^{-1})	K_i^{app} (nM)
1	48	—[c]	—	—
2	1.0	—	—	—
3	30	1.20	0.423	3.53
4	1.9	6.82	0.414	0.61
5	3.8	7.40	0.382	0.52

[a] The K_i-values are estimates obtained by steady-state analysis using pre-incubation of enzyme and inhibitor, as described in Experimental. [b] Obtained from the analysis of the enzyme inhibition data presented in Fig. 6, using eqn (3) and (4). k_{on} was determined from k_{off} and K_i^{app}, using the relationship $k_{on} = k_{off}/K_i$. The reaction was started by addition of enzyme. [c] —: not measured.

By injection of compound **1** at saturating concentrations, the apparent binding capacity of the sensor surface was estimated to be 40% of the theoretical maximum binding capacity. However, the sensor surface was not stable. This is illustrated in Fig. 2 where a baseline drift can be observed in sensorgrams before injection of compound **1**, and after dissociation of the compound. Still, the surface was stabilized with time, as illustrated by the difference in drift in the late dissociation phase for **1** when injected over the same surface but with a one hour time difference (Fig. 2a). The drift was higher at high surface densities and appeared to be correlated with the activity of MMP-12 as it was also found to be analyte-dependent, *i.e.* the injection of inhibitor caused a shift of the baseline corresponding to interrupted drift during the association phase (Fig. 2b).[13] To ensure that surfaces had sufficiently high binding capacities and stabilities over time for the performed experiments, a number of measures were taken, these include: (1) addition of 10 mM $CaCl_2$ to all reagents injected during the immobilisation procedure to ensure adequate immobilization levels, (2) the use of a cross-linking procedure and high concentrations of $CaCl_2$ in the running buffer (200 mM) to minimize the drift, (3) as low as possible surface densities and stabilization of the surface for one hour before experiments to avoid the initial rapid drift of new surfaces. The remaining drift was compensated for in the data analysis by subtraction of blank-injection responses from the analyte response.

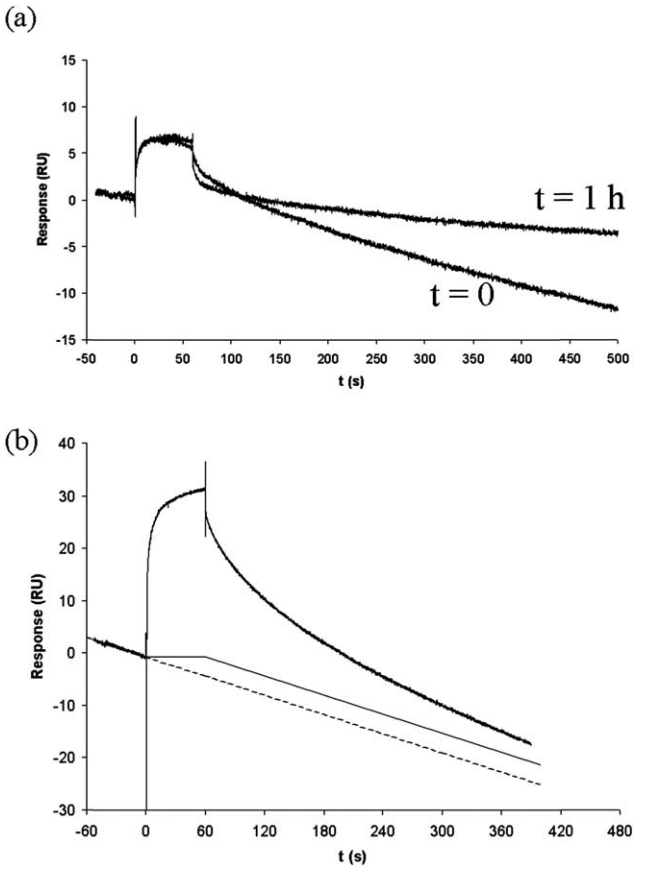

Fig. 2 Analysis of the stability of the MMP-12 sensor surface. (a) Effect of time on the baseline drift. Sensorgrams of 5 μM **1** injected over the same surface but with one hour difference. The first injection was made one hour after immobilization. (b) Effect of inhibitor on the baseline drift. Sensorgram of 5 μM **1**. The dashed line is an extrapolation of the baseline prior to injection. The solid line has the same slope, but is horizontal during association.

Immobilized MMP-12 was confirmed to be catalytically active by incubation of the substrate on a complete chip surface with an enzyme manually immobilized (*i.e.* outside the instrument). By docking the chip in the instrument before and after immobilization, it was determined that the signal increased by 2610 ± 300 RU, averaged over all four flow cells. This corresponds to 130 ng enzyme immobilized on the whole chip surface. The specific activity of the immobilized protein was 0.07 μmol min^{-1} mg^{-1}, while that of MMP-12 in solution was 0.7 μmol min^{-1} mg^{-1}.

Experimental design

Once the hydroxamate containing compounds (**2–5**) were tested, it was obvious that the original regeneration conditions were inadequate. For the purpose of identifying efficient regeneration procedures also for these compounds, a variety of conditions were tested, including salts, acids, bases, organic solvents, detergents, metal complexing agents and combinations thereof. Unfortunately, the repertoire of regeneration procedures that could be used was seriously restricted by the requirement of $CaCl_2$, combined with the high affinity of some inhibitors. Suitable regeneration conditions could therefore not be established for all compounds. This had serious practical consequences since the conventional serial experimental strategy using a single surface for a series of inhibitor injections could not be used – compounds with very slow dissociation rates could simply not be removed from the surface without damaging the surface itself. Thus, injection of such compounds blocked the surface and prohibited its further use. Although single cycle kinetics is sometimes useful when robust regeneration conditions are lacking, it was not attempted since the combination of very slow dissociation and analyte dependent drift was considered to prohibit the accurate quantification of rate constants also with that type of experimental design.[14] Instead, a new enzyme surface was thus prepared for every inhibitor used, and the resulting sensorgrams were qualitatively compared by overlaying the sensorgrams, normalised with respect to the reference compound **1**. It limited the possibility of obtaining quantitative data and resulted in a rather costly consumption of sensor chips. But, importantly, it provided useful data for qualitative comparative analysis of the different compounds.

Interaction kinetic characteristics of inhibitors

All of the selected hydroxamate containing compounds had very slow dissociation rates compared to the non-hydroxamate containing compound (Fig. 3). In order to verify that the hydroxamate-ZBG was the structural element responsible for the slow dissociation, a structural analogue to **1** (compound **2**) differing only by having a hydroxamate-ZBG instead of a carboxylate-ZBG (Fig. 1) was also tested. When injecting

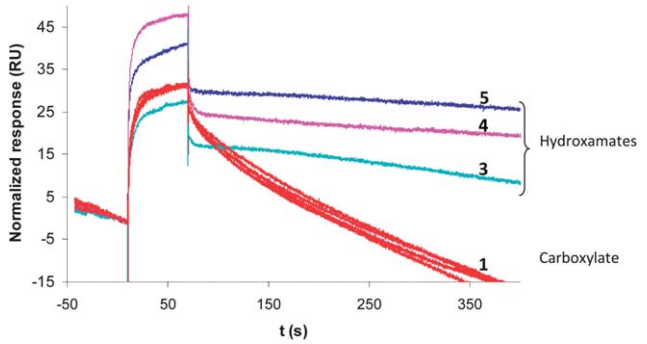

Fig. 3 Qualitative comparison of sensorgrams for inhibitors interacting with MMP-12. Sensorgrams of **3**, **4** and **5** were obtained with different enzyme surfaces, while one sensorgram of **1** was obtained for each surface and used to normalize the binding capacities of the different surfaces. All inhibitors were injected at a concentration of 5 μM. The sensorgrams are solvent corrected, adjusted for differences in molecular weight of inhibitors and blank subtracted.

compounds **1** and **2** at the same concentration, it was clearly shown that the hydroxamate compound had a much slower dissociation rate than the carboxylate compound (Fig. 4). As a result, the hydroxamate compound also had a higher steady-state level of binding, indicating that larger amounts of the complex were formed.

The sensorgrams for the studied compounds were distinctly biphasic, in both the association phase and the dissociation phase (Fig. 3), indicating an interaction mechanism involving more than one equilibrium. In an attempt to establish the nature of the complex interaction mechanism for the hydroxamate containing inhibitors, a more extensive experimental design using a series of inhibitor concentrations was used for compounds **1** and **5** (Fig. 5). For **5** the same strategy as used above, *i.e.* with new enzyme surfaces for each concentration, was exploited (Fig. 5a), while for compound **1**, the same sensor surface could be used for all concentrations since the inhibitor dissociated completely (Fig. 5b). These sensorgram series showed the biphasic characteristic for every concentration, perhaps most visible in the dissociation phase where **5**

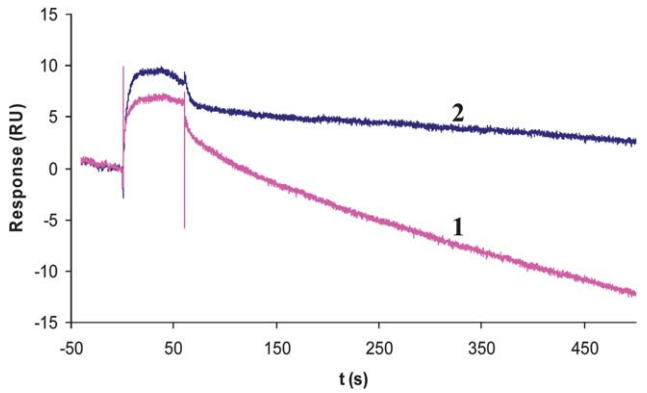

Fig. 4 Comparison of sensorgrams of hydroxamate- and a carboxylate-based inhibitor interacting with MMP-12 (compounds **1** and **2**, respectively). The inhibitors were injected at a concentration of 5 μM.

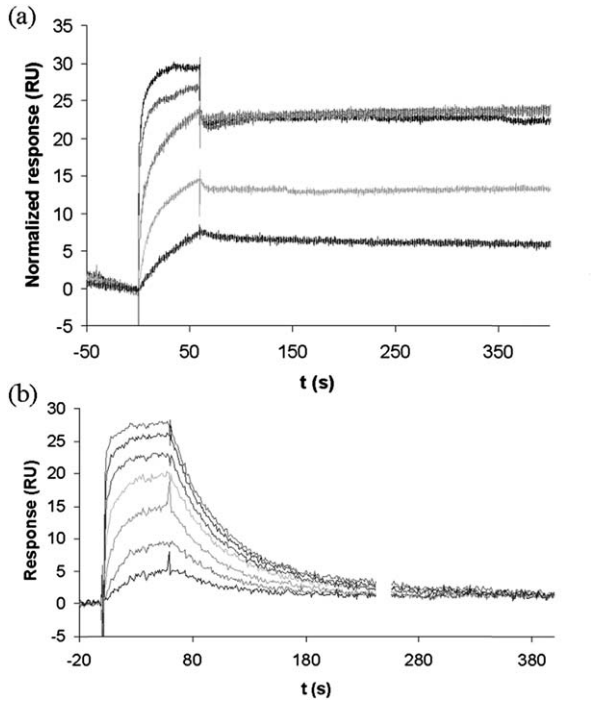

Fig. 5 Sensorgrams illustrating the concentration dependence of inhibitors interacting with MMP-12. (a) **5** at concentrations of 80 nM to 10 μM. (b) **1** at concentrations of 0.062–45 μM. The sensorgrams are solvent corrected, blank subtracted and adjusted for differences in binding capacity of the surfaces.

dissociates rapidly in the first ten seconds and thereafter the dissociation almost ceases. The highest concentrations of **5** also completely stopped the baseline-drift. Although both compounds **1** and **5** interacted with the enzyme in a concentration dependent manner, the two sets of sensorgrams differed qualitatively. None of the interactions could be satisfactorily described by a binding equation corresponding to a simple Langmuir or a 2-step interaction (*e.g.* induced fit), suggesting that the interaction is more complex. Other datasets (data not shown) suggested that the interaction was heterogeneous and composed of a high affinity and a low affinity component, perhaps resulting from auto-hydrolysis on the surface. But it was not possible to reliably determine the rate constants or affinities for these interactions. We therefore chose to keep the analysis qualitative, as it was sufficient to conclude for the purpose of the present study that the hydroxamate (but not the carboxylate) containing inhibitors dissociated very slowly from MMP-12.

Analysis of time-dependent inhibition

As a control, an alternative assay, involving measurement of the effect of the inhibitors on the catalytic activity of MMP-12 was used to verify the kinetic features of the inhibitors also in the solution. In such an assay the slow dissociation of the hydroxamate containing inhibitors from the enzyme (seen in Fig. 3–5) should be manifested as time-dependent inhibition, unless the inhibitor is pre-equilibrated with the enzyme for an extended time.[15] Therefore, the inhibition of MMP-12 by the three

slow-dissociating inhibitors (**3**, **4** and **5**) and the fast-dissociating carboxylate compound (**1**) was further investigated using an enzyme inhibition assay where enzyme was added to start the reaction (*i.e.* without pre-incubating the enzyme with the inhibitor).

These experiments showed that the three hydroxamate compounds displayed time-dependent inhibition, whereas the carboxylate compound did not (Fig. 6). An inhibitor concentration equal to the enzyme concentration was enough for complete inhibition by compounds **4** and **5**, indicating that the inhibition was due to an interaction with a 1 : 1 stoichiometry. A model for time-dependent inhibition was fitted to the data by non-linear regression in order to identify the mechanism for the observed time-dependent inhibition. The model for a simple 1 : 1 interaction ($E + I \rightleftharpoons EI$) resulted in satisfactory fits to the progress curve data of the time dependent inhibitors and allowed estimation of the kinetic parameters for compounds **3**, **4** and **5** (Table 1). (This procedure could not be applied for compound **1** since it was not time-dependent and other information required for estimation of K_i was lacking.) These K_i-values were lower than those initially determined by assuming competitive inhibition and using the integrated form of the Michaelis–Menten equation (Table 1). This reflects the differences in values obtained by a procedure based on analysis of complete progress curves and when pre-equilibrating the inhibitor with the enzyme so that the measurements are performed at a presumed steady-state.

Correlation between interaction kinetics, inhibition and structure

The three most inhibitory compounds (**2**, **4** and **5**) had similar apparent K_i-values (1.0, 1.9 and 3.8 nM, respectively) but differed clearly in the maximal level of the formed complex (Fig. 3). The two least effective inhibitors (**1** and **3**) had apparent K_i-values in the same range (48 and 30 nM, respectively) but quite different interaction profiles, with **1** dissociating relatively rapidly and **3** forming comparatively stable complexes, albeit not as efficiently as, for example, compound **4**. These comparisons show that there is no simple correlation between the interaction kinetics and the inhibitory parameter that could be determined for the compounds, indicating that the interaction characteristics are not easily understood simply from inhibition data, and *vice versa*. In contrast, the interaction kinetic profiles revealed a unique behaviour for the carboxylate compound, the only one showing clear dissociation. This illustrates the usefulness of time-resolved data and some of the problems in using enzyme inhibition analysis for characterization of enzyme inhibitor interactions.

Discussion

The original aim of the current study was to explore the kinetic features of hydroxamate containing MMP-12 inhibitors in order to better understand the relationship between the structure and

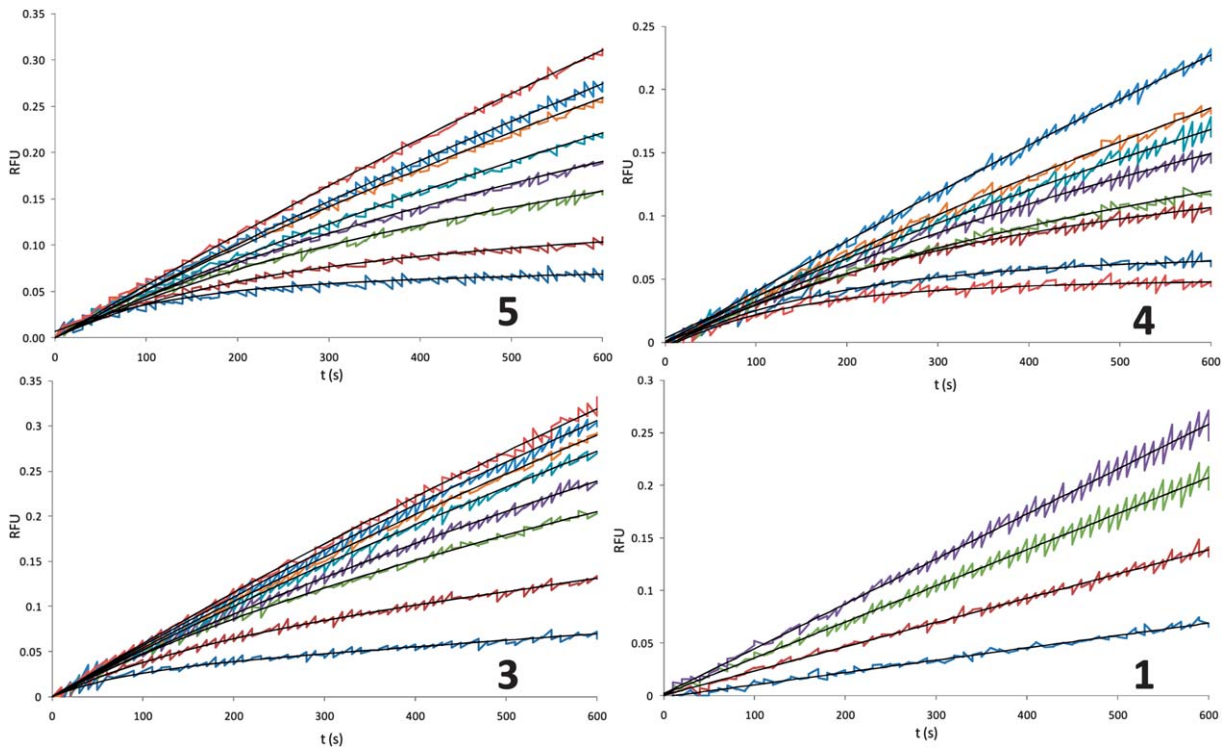

Fig. 6 Time dependence of MMP-12 inhibition. Progress curves with four different inhibitors: **1** at 0–100 nM, **3** at 0–100 nM, **4** at 0–10 nM and **5** at 0–10 nM. Each curve is the result of two measurements, *i.e.* the apparent noise represents the difference between the two replicate experiments. The black lines represent a fit of a model for time dependent inhibition, except for **1** which is a linear fit.

efficacy of inhibitors. A time-resolved biosensor assay was therefore used to study the interaction between MMP-12 and a small set of structurally diverse inhibitors, with and without a hydroxamate group. The assay was previously developed for screening of a fragment library[8] and required a slightly modified experimental design for the current experiments. The baseline drift was initially a problem but it could be minimized by optimization of the experimental procedure and compensated for in the data analysis by subtraction of blank injections from analyte injection sensorgrams. Instead, it was rather an interesting phenomenon that provided information about the characteristics of the immobilized enzyme. The drift was nearly abolished by injection of inhibitors of high affinity, suggesting that it was caused by autohydrolysis and that the immobilized enzyme was highly active. The same phenomenon has previously been observed when inhibitors bind to HIV-1 protease.[13] Furthermore, it was reduced by high calcium concentrations, which is in agreement with a recent study that suggests that calcium stabilizes the active form of the enzyme by preventing the partial unfolding necessary for autohydrolysis.[16] The cross-linking procedure used for stabilization of the surface also most likely prevented the unfolding of the enzyme that is required for autohydrolysis. The 10-fold lower activity of immobilized enzyme was somewhat puzzling, considering that the apparent functionality determined by the use of an inhibitor was approximately 40%. But the characteristics may be explained by considering the design of this experiment, where the substrate needs to be transported to the chip-surface in order to be hydrolysed. The limited mass transport of substrate to the immobilized enzyme in experiments performed with sensor chips simply sitting on the bench with "gentle agitation", *i.e.* without guaranteed adequate mixing, may reduce the effective concentration in the sensor matrix, thus reducing the observed specific activity on the chip. Nevertheless, the experiment showed that the immobilized enzyme was catalytically active although some catalytic power may have been lost in the immobilization procedure or after auto-hydrolysis after immobilization.

The interaction between the inhibitors and MMP-12 was found to be complex and not well described by a simple 1 : 1 interaction mechanism. Inhibitors containing a hydroxamate moiety were discovered to dissociate very slowly (if at all) from the enzyme–inhibitor complex. The inability to establish a regeneration procedure for these inhibitors required an unusual experimental design with one inhibitor injection per immobilization. Time-dependent inhibition is often observed with zinc-chelating MMP inhibitors, and it is in fact a general trait of reasonably potent inhibitors of MMPs,[15] although this is not immediately apparent when studying the literature since it is generally not recognized. Based on inhibition experiments, the mode of binding has been suggested to follow a simple one step interaction mechanism although there is evidence for a conformational change leading to a tighter enzyme–inhibitor complex.[17,18] The biosensor-data shows that the tested hydroxamate-based inhibitors had very slow dissociation rates when interacting with MMP-12, but the involvement of a rate limiting conformational change could not be confirmed. The combination of a complex interaction, slow dissociation, and a limited experimental dataset did not allow for the establishment of the interaction mechanism or a reliable quantification of the interaction kinetic rate constants, but the qualitative analysis provided the required information for this study.

The inhibition experiments confirmed the slow dissociation of the hydroxamates, which resulted in progress curves displaying characteristics typical of time dependent inhibition. Reliable quantification of the inhibition was not possible by this method either, even if rate constants and affinities of slow-binding inhibitors can in principle be determined by non-linear regression analysis of progress curves obtained at a series of inhibitor concentrations.[19] It becomes more challenging when the inhibitors are also tight-binding (see Morrison 1988 (ref. 20) and Copeland 2005 (ref. 15)), which was the case here. (The established terminology is somewhat misleading since "tight-binding" is defined as $K_i \leq [E]$ and depends on the assay setup rather than the value of K_i, while "slow-binding inhibitors" are not slow-binding *per se* (slow k_{on}), but the formation of complex (measured as time-dependence of inhibition) will appear to be slow when [I] is low since $k_{on} \times [I]$ will be very small even if k_{on} is as fast as diffusion permits.) But the regression analysis of the inhibition data did not give satisfactory fits even when accounting for both slow and tight binding. This might be due to a lower than expected, or decreasing, active enzyme concentration during measurements. It is also possible that the complex interaction seen in the biosensor assay is not well modelled by these equations. It was however possible to fit a simpler equation to the data, not accounting for tight-binding, which provided estimates of the parameters. Despite these limitations, this analysis provided more relevant inhibition constants than the steady-state analysis initially used (only resulting in K_i^{app}) and confirmed that the slow-dissociating hydroxamate inhibitors were time dependent inhibitors, whereas the carboxylate was not.

Although determination of the mechanism and kinetic parameters of slowly dissociating inhibitors is challenging also with a biosensor-based approach, it allows a semi-quantitative analysis that is very informative. In our earlier studies we have used different methods for elucidating the interaction mechanism and for the ranking of compounds on the basis of alternative parameters describing relevant kinetic features. For example, in the case of non-nucleoside inhibitors interacting with HIV-1 reverse transcriptase (NNRTIs),[21] a comparative analysis of different compounds and simulation of sensorgrams provided approximations of the range of the kinetic constants and enabled an interpretation of the kinetic features of relevance for anti-replicative efficacy in the cell culture. This procedure could not be used here due to the uncharacterized complexity of the interaction (not shown).

One of the advantages of time-resolved analysis of molecular interactions is that it provides more direct information about the interaction between the inhibitor and its target than conventional enzyme inhibition assay methods used for lead discovery. For example, the irreversible/slow dissociating nature of lead compounds is readily observed by this biosensor-based approach, but can be missed or misinterpreted by conventional

procedures that need to be designed specifically for detection of this feature. When using a biosensor-based approach, there is no risk that the slow-binding detected in an inhibition assay is mistaken for slow association since it will be clearly seen as slow dissociation. Moreover, the direct readout makes it independent on substrate-related effects, which can be problematic when comparing data for different enzymes. In the case of hydroxamate-based MMP inhibitors, the lack of catalysis-independent inhibitor kinetic information may have led to misleading interpretations of compound selectivity, one of the main problems associated with hydroxamate compounds. It will therefore briefly be elaborated here:

The most common methods for evaluating structure activity relationships and selectivity for MMP inhibitors are based on IC_{50}- or K_i-values obtained by initial rate measurements of enzyme inhibition using FRET-peptide substrates.[22] There are several concerns with this approach. Firstly, it assumes that the enzyme and the inhibitor are in rapid equilibrium during the measurements, or that they have reached equilibrium in a pre-incubation step. It is not trivial to establish for inhibitors with very slow association and/or slow dissociation rates of inhibition, or that follow a complex inhibition mechanism. Secondly, analysis of selectivity with respect to target analogues (*e.g.* MMP isoenzymes) requires that the assays and/or the data are normalized with respect to differences in the catalytic efficacy of the enzymes, accounting for example for differences in the K_M-values for the enzymes and substrates used. Failing to recognize these issues can, for example, result in the common, but misleading, comparisons of IC_{50}-values for different enzymes. A typical example is a study that intends to show the selectivity profile of compound **5**.[23] However, it has not recognized the slow dissociation of this class of inhibitors, calling for an experimental design and analysis procedure that takes this into consideration. In addition, it uses the same substrate and conditions for all MMPs studied, without accounting for the different catalytic properties of the isoenzymes. The use of IC_{50}-values for the "selectivity" analysis of compound **5** in the study is therefore problematic. These considerations also explain why the apparent K_i-values obtained in the present study were not useful for description of the affinity of the studied compounds and why there was no simple correlation between the interaction kinetic and the inhibition data.

By interpreting the data into the context of selectivity we illustrate that it is easy to misinterpret inhibition data without substrate-independent interaction kinetic information, *i.e.* association and dissociation rate constants. But more importantly, without kinetic information it is not possible to fully understand structure–activity relationships and to modify inhibitor structures so that both affinity and residence time are optimized.

The data supports the hydroxamate-based design of MMP inhibitors, in the sense that this clearly results in very effective inhibitors. The interactions between hydroxamates and zinc in solution have been explored, providing a good description of the interaction between this moiety and the active site of the enzyme.[24] However, additional interactions, for example with the S1′-pocket, are also needed in order to result in inhibitors with slow dissociation rates. Such interactions can also ensure that binding only occurs to the specific MMP of interest since hydroxamate-containing compounds can in principle interact with all MMP isoenzymes and potentially with many other enzymes that have catalytically essential zinc ions. Alternative strategies of achieving selectivity for compounds with strong ZBGs have been suggested; where one postulates that the slow binding behaviour of these inhibitors can be utilized to gain selectivity.[25] Since our data shows that the slow-binding behaviour is an artifact caused by slow dissociation rather than being an effect of slow association, this strategy is not realistic. Another line of development that is pursued, is to exclude the ZBG altogether and focus on inhibitors binding in the S1′-specificity loop.[26] This is difficult since the active site of MMPs is flexible and the S1′-specificity loop is mobile.[27] Hence, whatever strategy is used, structural modelling (for example using available crystal structures[28,29]) and design need the support of interaction kinetic information in order to analyse specificity issues. However, this requires full insight into the interaction mechanism. In a recent study involving non-nucleoside inhibitors of HIV-1 reverse transcriptase, we have shown that slow dissociation as such is not the critical parameter for efficacy, but that other kinetic features are also important.[21] Thus, it is not possible to use a simple and general rule-of-thumb for the desirable kinetic features of inhibitors (such as slow k_{off} or long residence time[30]). The ideal features but must be established on a case-by-case basis. The biosensor assay presented herein can clearly provide the detailed kinetic information that can help guide the design of a new generation of specific and efficient MMP inhibitors. We have already exploited the biosensor assay described herein for screening of a fragment library and identified inhibitors that do not contain zinc-chelating groups.[8] Further development of these hits into leads is currently being explored.

Conclusions

The present study provides new insights into the structural and kinetic features of effective MMP-12 inhibitors and that biosensor-based interaction analysis is very informative for lead characterization, especially for slowly dissociating inhibitors where enzyme inhibition-based assays have several drawbacks. The data show that non-covalent, but slowly dissociating inhibitors may have the same problems as covalent modifiers. This puts the recent focus on long residence time of drugs[30] in a new perspective and demonstrates the importance of characterizing the mechanism and kinetics of inhibitors.

Experimental

Inhibitors

Compounds **3** (ref. 9) and **4** (ref. 10) were obtained from Calbiochem (EMD Chemicals, Gibbstown, NJ, USA) and compound **5** (ref. 11 and 12) (GM 6001, ilomastat) from Chemicon (Millipore, Solna, Sweden). The purity of all tested compounds was ≥95%, as determined by analytical high-performance liquid chromatography (HPLC).

Chemical procedures

General. NMR-spectra were recorded on a Varian 500 MHz instrument using $(CD_3)_2SO$ as a solvent. Tetramethylsilane (TMS) was used as reference.

LC-MS purity measurements were performed with a Waters Alliance 2695 HPLC instrument and a 50 × 3.0 mm ACE C_8 column with 3 μm particles and two different methods. *Chromatography system A*. Mobile phases A: 10 mM NH_4OAc, B: 10 mM NH_4OAc in 90% CAN; gradient program: 20–100% B in 5 min followed by a wash for 2 min at 100% B; flow rate: 0.8 mL min^{-1}; injection volume: 5 μL; sample concentration: 1 mg mL^{-1} (diluted in acetonitrile, ACN); detection: UV @ 210–400 nm and ESI-MS. *Chromatography system B*. Same as system A except: mobile phases A: 0.2% formic acid; B: 0.18% formic acid in ACN; sample concentration: 1 mg mL^{-1} (diluted in MeOH).

The mass spectrometry analyses were performed on a Waters ZQ instrument equipped with an electrospray interface. The operating conditions for the electrospray interface and the mass spectrometer were spray voltage 3300 V, cone voltage 30 V, source temperature 120 °C, desolvation gas temperature 300 °C, and desolvation gas flow 800 L h^{-1}. Full scan mass spectra of positive ions were recorded for the mass range 300–900 Da (300–700 Da for **2**). The scan time was 1.0 s per spectrum. All data were processed using the Masslynx software version 4.1 from Waters.

LC-MS accurate mass measurements were performed using a HDMS Synapt instrument from Waters (UK) equipped with a lockspray interface, connected to a Waters Aquity system. The acquisition range was *m*/*z* 100 to 1000 with an acquisition time of 0.15 s (+ESI). Leucine enkephalin was used as lock mass. The reversed phase column was an YMC-UltraHT Pro C_{18}, 2.1 × 50 mm, 2 μm, 120 A from YMC (U.S.A) and the mobile phases were based on water/acetonitrile containing 0.2% formic acid.

(*S*)-4-Benzyl-3-(4-(4-bromophenyl)butanoyl)oxazolidin-2-one (6). Under nitrogen, to a solution of Evan's auxiliary (*S*)-4-benzyloxazolidin-2-one (708 mg, 4.0 mmol) in dry tetrahydrofuran (THF) (15 mL) at −78 °C was added *n*-BuLi (2.5 mL, 1.6 M, 4.0 mmol). The mixture was stirred at −78 °C for 30 min, where after 4-(4-bromophenyl)-butyryl chloride (877 mg, 4.05 mmol) in THF (5 mL) was added slowly. After stirring for another 1 h, the reaction was allowed to warm to room temperature, and stirred for additional 6 h, and finally quenched with saturated aqueous NH_4Cl. The aqueous phase was extracted with CH_2Cl_2; the combined organic layers was washed with aqueous $NaHCO_3$ and brine, dried over Na_2SO_4, and concentrated under reduced pressure. The residue was purified by silica gel column chromatography to provide the compound **6** in 83% yield (1335 mg).

(*R*)-*tert*-Butyl 3-((*S*)-4-benzyl-2-oxooxazolidine-3-carbonyl)-5-(4-bromophenyl) pentanoate (7). Under nitrogen, to a solution of **6** (804 mg, 2.0 mmol) in dry THF (10 mL) at −78 °C was added freshly prepared lithium diisopropylamide (LDA) in THF (2.1 mmol). The mixture was stirred at −78 °C for 1 h, where after *tert*-butyl bromoacetate (429 mg, 2.2 mmol) was added. The reaction was continued to stir for another 2 h at −78 °C, and then allowed to warm to room temperature overnight. Saturated aqueous NH_4Cl was added and THF was removed under reduced pressure. The residue was diluted with EtOAc and washed with brine. The organic layer was dried over Na_2SO_4, and concentrated under reduced pressure. The crude product was purified by silica gel column chromatography to give **7** in 74% yield (764 mg).

(*R*)-2-(4-Bromophenethyl)-4-*tert*-butoxy-4-oxobutanoic acid (8). To a solution of **7** (671 mg, 1.3 mmol) in THF–H_2O (4/1, 10 mL) at 0 °C was added hydrogen peroxide (30%, 0.7 mL). After stirring for 10 min, lithium hydroxide (62 mg, 2.6 mmol) was added. The reaction was stirred overnight and then quenched with Na_2SO_3. THF was evaporated under reduced pressure. The pH of aqueous solution was adjusted to 2 with HCl (1 N), extracted with EtOAc and washed with brine. The organic layer was dried over Na_2SO_4, and concentrated under reduced pressure. The residue was purified by silica gel column chromatography to afford the compound **8** in 85% yield (394 mg). ^{1}H-NMR (300 MHz, $CDCl_3$): δ 7.42 (d, $J = 8.4$ Hz, 2H), 7.07 (d, $J = 8.4$ Hz, 2H), 2.90–2.78 (m, 1H), 2.73–2.58 (m, 3H), 2.47–2.38 (m, 1H), 2.05–1.95 (m, 1H), 1.94–1.72 (m, 1H), 1.44 (s, 9H).

(*R*)-*tert*-Butyl 5-(4-bromophenyl)-3-((*S*)-1-(methylamino)-1-oxo-3-phenylpropan-2-ylcarbamoyl)pentanoate (9). To a solution of **8** (357 mg, 1 mmol) in dimethylformamide (DMF) (5 mL) was added hydroxybenzotriazole (HOBt) (270 mg, 2 mmol) at 0 °C. The mixture was cooled to −15 °C, and EDC (384 mg, 2 mmol) was added. After 30 min, the reaction was warmed to room temperature, L-phenylalanine methylamide hydrochloride (428 mg, 2 mmol) and *N*-methylmorpholine (NMM) (0.16 mL, 1.44 mmol) were added. The mixture was stirred overnight. The solvent was removed and the residue was partitioned between ethyl acetate (EtOAc) and saturated NH_4Cl solution. The aqueous layer was extracted with EtOAc. The combined organic layers were dried and concentrated under reduced pressure. The residue was purified by silica gel column chromatography to afford **9** in 72% yield (372 mg). ^{1}H-NMR (300 MHz, $CDCl_3$): δ 7.38 (d, $J = 8.7$ Hz, 2H), 7.34–7.20 (m, 5H), 6.98 (d, $J = 8.1$ Hz, 2H), 6.38 (d, $J = 8.1$ Hz, 1H), 5.80 (br, s, 1H), 4.52 (dd, 1H), 3.12–3.05 (m, 2H), 2.71 (d, $J = 2.4$ Hz, 3H), 2.57–2.34 (m, 5H), 1.92–1.82 (m, 1H), 1.43 (s, 9H).

(*R*)-*tert*-Butyl 3-((*S*)-1-(methylamino)-1-oxo-3-phenylpropan-2-ylcarbamoyl)-5-(4-(pyridin-3-yl)phenyl)pentanoate (10). Under nitrogen, the mixture of **9** (350 mg, 0.68 mmol), 3-pyridineboronic acid (120 mg, 0.82 mmol), $Pd(PPh_3)_4$ (39 mg, 0.034 mmol), 2 M Na_2CO_3 (1 mL), toluene (5 mL), and EtOH (3 mL) was heated to reflux for 2 h. The EtOH was removed and the residue was diluted with CH_2Cl_2, washed with brine, dried and concentrated under reduced pressure. The crude product was purified by silica gel column chromatography to give **10** in 74% yield (260 mg).

(*R*)-3-((*S*)-1-(Methylamino)-1-oxo-3-phenylpropan-2-ylcarbamoyl)-5-(4-(pyridin-3-yl)phenyl)pentanoic acid (1). To a solution of **10** (258 mg, 0.5 mmol) in CH_2Cl_2 (5 mL) at 0 °C were added trifluoroacetic acid (TFA) (2 mL) and water (3 drops). After stirring for 3 h at room temperature, the mixture was diluted with EtOAc and 10% NaOH was added to adjust the pH to 6. The aqueous layer was extracted with EtOAc, the combined organic phases were dried over anhydrous Na_2SO_4 and concentrated under reduced pressure. The crude product was purified by

silica gel column chromatography to afford **1** in 92% yield (211 mg).

^{1}H-NMR (500 MHz, DMSO-d_6) δ 9.04 (s, 1H), 8.70 (d, 1H, J = 5.2 Hz), 8.43 (d, 1H, J = 8.0 Hz), 8.11 (d, 1H, J = 7.6 Hz), 7.82 (dd, 1H, J = 4.2; 8.9 Hz), 7.77 (dd, 1H, J = 5.2; 8.0 Hz), 7.70 (d, 2H, J = 8.4 Hz), 7.29 (d, 2H, J = 8.4 Hz), 7.26–7.15 (m, 5H), 4.47 (td, 1H, J = 6.2; 9.4; 14.6 Hz), 2.98 (dd, 1H, J = 6.2; 14.7 Hz), 2.85 (dd, 1H, J = 10.2; 14.7 Hz), 2.68 (m, 1H), 2.58 (d, 3H, J = 4.2 Hz), 2.50 (m, 2H), 2.41 (dd, 1H, J = 8.0, 16.3 Hz), 2.25 (dd, 1H, J = 6.7, 16.3 Hz), 1.68 (m, 2H); ^{13}C-NMR (125 MHz, DMSO-d_6) δ 173.9, 173.7, 171.9, 145.0, 144.4, 143.5, 138.5, 138.5, 137.4, 133.4, 129.6 (2C), 128.5–126.6 (7C), 125.9, 54.5, 41.7, 37.9, 36.6, 34.3, 32.6, 26.0. HRMS: $(M + H)^+$ calculated: 460.2236, found; 460.2242. LC-UV purity system A t_R: 2.43 min, 98.8%.

(*R*)-*N*^{4}-Hydroxy-*N*^{1}-((*S*)-1-(methylamino)-1-oxo-3-phenylpropan-2-yl)-2-(4-(pyridin-3-yl)phenethyl)succinamide (2). To a solution of the above obtain compound **1** (150 mg, 0.33 mmol) in DMF (5 mL) was added *N*-methylmorpholine (NMM) (0.16 mL, 1.38 mmol). The mixture was cooled to 0 °C and benzotriazole-1-yl-oxy-tris-(dimethylamino)-phosphonium hexafluorophosphate (BOP) (165 mg, 0.38 mmol) was added. The reaction mixture was stirred for 30 min at 0 °C, where after hydroxylammonium chloride (48 mg, 0.69 mmol) was added. The reaction was allowed to warm to room temperature and stirred overnight. The reaction mixture was concentrated under reduced pressure. The residue was diluted with EtOAc, washed with 1 N HCl, saturated $NaHCO_3$ and brine, dried over anhydrous Na_2SO_4, and concentrated under reduced pressure. The residue was purified by silica gel column chromatography to afford the product **2** in 68% yield (105 mg).

^{1}H-NMR (500 MHz, DMSO-d_6) δ 10.45 (s, 1H), 8.86 (d, 1H, J = 2.2 Hz), 8.77 (s, 1H), 8.54 (dd, 1H, J = 1.5; 4.6 Hz), 8.15 (d, 1H, J = 8.3 Hz), 8.04 (dd, 1H, J = 2.0; 8.0 Hz), 7.97 (q, 1H), 7.62 (d, 2H, J = 8.0 Hz), 7.46 (dd, 1H, J = 4.6; 8.0 Hz), 7.21 (d, 2H, J = 8.0 Hz), 7.26–7.16 (m, 5H), 4.46 (td, 1H, J = 5.2; 9.1; 14.3 Hz), 3.05 (dd, 1H, J = 5.0; 13.7 Hz), 2.84 (dd, 1H, J = 9.6; 13.7 Hz), 2.61 (m, 1H), 2.59 (d, 3H, J = 4.6 Hz), 2.44–2.38 (m, 2H), 2.10 (dd, 1H, J = 7.2, 14.8 Hz), 2.01 (dd, 1H, J = 8.2, 14.8 Hz), 1.65–1.57 (m, 2H); ^{13}C-NMR (125 MHz, DMSO-d_6) δ 173.9, 172.0, 168.0, 148.7, 147.9, 142.5, 138.7, 135.9, 135.0, 134.3, 129.5 (2C), 128.5–126.6 (7C), 124.3, 54.6, 42.4, 37.7, 36.4, 33.9, 32.6, 26.1. HRMS: $(M + H)^+$ calculated: 475.2345, found: 475.2337. LC-UV purity system B t_R: 2.60 min, 99.0%.

Enzyme

Pure recombinant human MMP-12 was produced essentially as described by Morales *et al.*[31] The protein consisted of the catalytic domain, comprising amino acids 100–263 of the entire naturally translated pre-protein.

Interaction experiments

A Biacore S51 instrument (Biacore AB/GE Healthcare Biosciences, Uppsala, Sweden) was used for all experiments, except for the characterisation of compound **1** interactions, which were performed with a Biacore 2000 instrument. The assay was performed according to the procedures previously described by Nordström *et al.*[8] MMP-12 was immobilized on a CM5 chip using amine coupling. The flow rate was 10 μL min^{-1} during the immobilization procedure. The chip was activated by an injection of EDC/NHS for ten minutes. MMP-12, at a concentration of 60 μg mL^{-1} in 10 mM maleate, pH 6.0, 10 mM $CaCl_2$, was subsequently injected for seven minutes. A cross-linking step[32] consisting of a three-minute injection of EDC/NHS, containing 10 mM $CaCl_2$, followed by a deactivation injection during ten minutes of 1 M ethanolamine, pH 8.5, 10 mM $CaCl_2$ concluded the immobilization procedure. The running buffer during immobilization was 10 mM Hepes, pH 7.4, 0.2 M $CaCl_2$, 0.1 M NaCl with 0.005% surfactant P-20.

The running buffer for the interaction experiments was 50 mM Tris–HCl, pH 7.4, 0.2 M $CaCl_2$, 0.1 M NaCl, 0.005% surfactant P-20, 5% DMSO. Solvent correction solutions were prepared from running buffer with 4.5% and 5.8% DMSO stock solutions, as described in the Biacore S51 methodology handbook (Biacore AB/GE Healthcare Biosciences, Uppsala Sweden).

Inhibition assay

The enzyme activity was measured in 96-well plates (Corning/Sigma Aldrich, Sweden) at a final volume of 150 μL, where 10 μL of 3 M $CaCl_2$ dissolved in H_2O, 115 μL of buffer (50 mM Tris, pH 7.5), 5 μL of inhibitor dissolved in DMSO, and 10 μL of the internally quenched fluorogenic peptide substrate Mca-Pro-Leu-Gly-Leu-Dpa-Ala-Arg-NH_2 (RnD Systems Europe Ltd) dissolved in buffer with 12.5% DMSO to 750 μM, were added to the wells. This was incubated at 30 °C for 5 minutes before the reaction was started by adding 10 μL of 3 μg mL^{-1} MMP-12. The final concentration of $CaCl_2$ was 200 mM, while the final concentration of DMSO was 4.2% (v/v) and that of MMP-12 and the substrate was 10 nM and 50 μM respectively. The enzyme stock solution (Tris buffer pH 7.5, 5 mM $CaCl_2$) was diluted in assay buffer just prior to starting the reaction. Plates were read on a Fluoroskan Ascent (Thermo Labsystems Oy, Helsinki, Finland) using λ_{ex} = 320 nm and λ_{em} = 460 nm for 25 minutes.

Apparent K_i-values were determined using slightly different conditions and the assay set-up: the assay was performed at room temperature in 200 mM calcium acetate, 50 mM Tris–HCl, pH 7.5, 1% DMSO, 50 μM substrate and 2 nM enzyme. The addition of substrate started the reaction after a pre-incubation of enzyme and inhibitor for 10 minutes. The plates were read for 12 minutes.

In order to measure the activity of the immobilized enzyme, it was immobilized manually to the entire surface of a CM5 chip outside the instrument, using the same procedure as described above with the S51-instrument. The substrate (60 μL of 50 μM in running buffer) was subsequently pipetted as a droplet to the surface. After 20 minutes under gentle agitation at room temperature, the substrate droplet was transferred to a 96-well plate and fluorescence was measured, as described above. The amount of immobilized protein was quantified according to Stenberg *et al.*[33]

Data analysis

Biacore S51 software and/or Biaevaluation 3.2 (Biacore AB/GE Healthcare Biosciences, Uppsala, Sweden) were used for

evaluating the biosensor data. The response of a blank sample injection following the analyte injection was subtracted from the analyte response. The analyte response was then normalized with respect to the response from a positive control.

Apparent K_i-values were determined from product *vs.* time data (entire progress curves) by fitting of the integrated Michaelis–Menten equation:[34]

$$[\mathrm{P}] = S_0 - K_\mathrm{M} W\left\{\frac{S_0}{K_\mathrm{M}} \mathrm{e}^{\left(\frac{S_0 - Vt}{K_\mathrm{M}}\right)}\right\} \quad (1)$$

where W is a Lambert's Omega function which satisfies the equations:

$$W(z) = y$$

$$y\mathrm{e}^y = z \quad (2)$$

The Lambert Omega function was implemented in SigmaPlot 2000 using 5 iterations of the algorithm of Corless *et al.*[35]

The time dependence of inhibition was evaluated in BIAevaluation 3.0.2 by fitting the following equation to product *vs.* time data:

$$[\mathrm{P}] = v_\mathrm{s} t + \left(\frac{v_\mathrm{i} - v_\mathrm{s}}{k_\mathrm{obs}}\right)\left(1 - \mathrm{e}(-k_\mathrm{obs} t)\right) \quad (3)$$

where

$$k_\mathrm{obs} = k_\mathrm{off}\left(1 + \frac{I}{K_\mathrm{i}}\right) \quad (4)$$

Acknowledgements

This work was supported by the Swedish Agency for Innovation Systems (VINNOVA) and the Swedish Research Council (VR). We would also like to thank Tatiana Agback (Medivir AB) and Kurt Benkestock (Medivir AB) for help regarding the analyses of **1** and **2**.

References

1 N. D. Rawlings, D. P. Tolle and A. J. Barrett, *Nucleic Acids Res.*, 2004, **32**, D160–D164.
2 G. L. Snider, *Am. J. Respir. Crit. Care Med.*, 2003, **167**, 1045–1046.
3 M. Liu, H. Sun, X. Wang, T. Koike, H. Mishima, K. Ikeda, T. Watanabe, N. Ochiai and J. Fan, *Arthritis Rheum.*, 2004, **50**, 3112–3117.
4 B. Turk, *Nat. Rev. Drug Discovery*, 2006, **5**, 785–799.
5 L. M. Coussens, B. Fingleton and L. M. Matrisian, *Science*, 2002, **295**, 2387–2392.
6 C. M. Overall and O. Kleifeld, *Br. J. Cancer*, 2006, **94**, 941–946.
7 C. M. Overall and O. Kleifeld, *Nat. Rev. Cancer*, 2006, **6**, 227–239.
8 H. Nordström, T. Gossas, M. Hämäläinen, P. Källblad, S. Nyström, H. Wallberg and U. H. Danielson, *J. Med. Chem.*, 2008, **51**, 3449–3459.
9 J. I. Levin, J. Chen, M. Du, M. Hogan, S. Kincaid, F. C. Nelson, A. M. Venkatesan, T. Wehr, A. Zask, J. DiJoseph, L. M. Killar, S. Skala, A. Sung, M. Sharr, C. Roth, G. Jin, R. Cowling, K. M. Mohler, R. A. Black, C. J. March and J. S. Skotnicki, *Bioorg. Med. Chem. Lett.*, 2001, **11**, 2189–2192.
10 S. Pikul, K. L. McDow Dunham, N. G. Almstead, B. De, M. G. Natchus, M. V. Anastasio, S. J. McPhail, C. E. Snider, Y. O. Taiwo, T. Rydel, C. M. Dunaway, F. Gu and G. E. Mieling, *J. Med. Chem.*, 1998, **41**, 3568–3571.
11 M. Yamamoto, H. Tsujishita, N. Hori, Y. Ohishi, S. Inoue, S. Ikeda and Y. Okada, *J. Med. Chem.*, 1998, **41**, 1209–1217.
12 D. E. Levy, F. Lapierre, W. Liang, W. Ye, C. W. Lange, X. Li, D. Grobelny, M. Casabonne, D. Tyrrell, K. Holme, A. Nadzan and R. E. Galardy, *J. Med. Chem.*, 1998, **41**, 199–223.
13 P. O. Markgren, M. Hamalainen and U. H. Danielson, *Anal. Biochem.*, 2000, **279**, 71–78.
14 R. Karlsson, P. S. Katsamba, H. Nordin, E. Pol and D. G. Myszka, *Anal. Biochem.*, 2006, **349**, 136–147.
15 R. A. Copeland, *Methods Biochem. Anal.*, 2005, **46**, 1–265.
16 T. Gossas and U. H. Danielson, *Biochem. J.*, 2006, **398**, 393–398.
17 G. Rosenblum, S. O. Meroueh, O. Kleifeld, S. Brown, S. P. Singson, R. Fridman, S. Mobashery and I. Sagi, *J. Biol. Chem.*, 2003, **278**, 27009–27015.
18 F. J. Moy, P. K. Chanda, J. Chen, S. Cosmi, W. Edris, J. I. Levin, T. S. Rush, J. Wilhelm and R. Powers, *J. Am. Chem. Soc.*, 2002, **124**, 12658–12659.
19 J. F. Morrison and C. T. Walsh, *Adv. Enzymol. Relat. Areas Mol. Biol.*, 1988, **61**, 201–301.
20 J. F. Morrison, *Biochim. Biophys. Acta*, 1969, **185**, 269–286.
21 M. Elinder, P. Selhorst, G. Vanham, B. Öberg, L. Vrang and U. H. Danielson, *Biochem. Pharmacol.*, 2010, **80**, 1133–1140.
22 C. Lombard, J. Saulnier and J. Wallach, *Biochimie*, 2005, **87**, 265–272.
23 R. Johnson, A. G. Pavlovsky, D. F. Ortwine, F. Prior, C. F. Man, D. A. Bornemeier, C. A. Banotai, W. T. Mueller, P. McConnell, C. Yan, V. Baragi, C. Lesch, W. H. Roark, M. Wilson, K. Datta, R. Guzman and H. K. Dyer, *J. Biol. Chem.*, 2007, **282**, 27781–27791.
24 M. Tegoni, F. Dallavalle and M. Amelia Santos, *J. Inorg. Biochem.*, 2004, **98**, 209–218.
25 M. M. Bernardo, S. Brown, Z. H. Li, R. Fridman and S. Mobashery, *J. Biol. Chem.*, 2002, **277**, 11201–11207.
26 A. C. Dublanchet, P. Ducrot, C. Andrianjara, M. O'Gara, R. Morales, D. Compere, A. Denis, S. Blais, P. Cluzeau, K. Courte, J. Hamon, F. Moreau, M. L. Prunet and A. Tertre, *Bioorg. Med. Chem. Lett.*, 2005, **15**, 3787–3790.
27 P. Cuniasse, L. Devel, A. Makaritis, F. Beau, D. Georgiadis, M. Matziari, A. Yiotakis and V. Dive, *Biochimie*, 2005, **87**, 393–402.

28 R. Lang, A. Kocourek, M. Braun, H. Tschesche, R. Huber, W. Bode and K. Maskos, *J. Mol. Biol.*, 2001, **312**, 731–742.
29 H. Nar, K. Werle, M. M. Bauer, H. Dollinger and B. Jung, *J. Mol. Biol.*, 2001, **312**, 743–751.
30 R. A. Copeland, D. L. Pompliano and T. D. Meek, *Nat. Rev. Drug Discovery*, 2006, **5**, 730–739.
31 R. Morales, S. Perrier, J. M. Florent, J. Beltra, S. Dufour, I. De Mendez, P. Manceau, A. Tertre, F. Moreau, D. Compere, A. C. Dublanchet and M. O'Gara, *J. Mol. Biol.*, 2004, **341**, 1063–1076.
32 P. O. Markgren, M. T. Lindgren, K. Gertow, R. Karlsson, M. Hämäläinen and U. H. Danielson, *Anal. Biochem.*, 2001, **291**, 207–218.
33 E. Stenberg, B. Persson, H. Roos and C. Urbaniczky, *J. Colloid Interface Sci.*, 1991, **143**, 513–526.
34 C. T. Goudar, J. R. Sonnad and R. G. Duggleby, *Biochim. Biophys. Acta*, 1999, **1429**, 377–383.
35 R. M. Corless, G. H. Gonnett, D. E. G. Hare, D. J. Jeffrey and D. E. Knuth, *Adv. Comput. Math.*, 1996, **5**, 329–359.

